

Detecting glucose-induced changes in *in vitro* and *in vivo* experiments with optical coherence tomography

Matti Kinnunen

Risto Myllylä

University of Oulu
Optoelectronics and Measurement Techniques Laboratory
and Infotech Oulu

Department of Electrical and Information Engineering
P.O. Box 4500

FIN-90014 Oulu, Finland

E-mail: matti.kinnunen@ee.oulu.fi

Seppo Vainio

University of Oulu

BioCenter Oulu

Laboratory of Developmental Biology

Department of Medical Biochemistry and Molecular
Biology

Faculty of Medicine, P.O. Box 5000

FIN-90014 Oulu, Finland

Abstract. Optical clearing is a well-known phenomenon. It is based on the matching of refractive indices of a bulk material and scattering particles. The same principle is also used in scattering-based optical measurements of different constituents, such as glucose. By registering changes in scattering, it is possible to evaluate changes in the concentration of a solvent. This work describes the use of optical coherence tomography (OCT) to monitor glucose-induced changes in the optical properties of samples. Intralipid™, mouse skin tissue, and mice (C57BL) are used as samples. Differences between *in vitro* and *in vivo* measurement conditions, the effect of glucose on the samples' optical properties, as well as possible problems in OCT experiments are discussed. A comparison of OCT signals from mouse skin samples and mice *in vivo* shows that the intensity of backscattered radiation is stronger in a living animal than in cultured tissue. Moreover, the effect of glucose on the scattering properties is larger in an *in vivo* case than in an *in vitro* case. In comparison with tissue, the effect of glucose is the smallest in Intralipid. The results increase the value of using cultured tissue in developing optical sensing techniques. © 2008 Society of Photo-Optical Instrumentation Engineers. [DOI: 10.1117/1.2904957]

Keywords: light scattering; glucose; refractive index; optical coherence tomography; tissue.

Paper 07076SSRR received Mar. 1, 2007; revised manuscript received Aug. 20, 2007; accepted for publication Aug. 24, 2007; published online Apr. 14, 2008.

1 Introduction

Turbid materials and biological tissues scatter light strongly. For this reason, the imaging depth of different optical techniques is quite limited in such media. Light scattering properties are determined by the size, position, and shape of the scattering particles in relation to the wavelength and direction of the probing light. The major cause of scattering is the refractive index mismatch between the scattering particles and the background medium. In tissue, these components (particles) are mitochondria, cytoplasm, cell membranes, extracellular media, and collagen and elastin fibers.¹⁻³ Seventy percent of the dry weight of skin consists of collagen fibers with a high refractive index, and hence the main scatterers are collagen fibers.^{2,4}

Optical clearing by means of immersion technology is a powerful tool for controlling the optical properties of tissues. It is based on matching of the refractive indices of the bulk material and scattering particles. Several clearing agents with different refractive indices have been used to decrease scattering, enhance light penetration depth, increase image contrast, and overcome the limitations of strong optical scattering of biological samples.⁵

A theoretical model has been developed to describe solvent penetration by diffusion and the matching of refractive indices in fibrous tissue. Permeation of the agents alters the size of scattering centers by contracting or swelling, which controls the rate of optical clearing.⁴

The optical clearing phenomenon also forms the basis for optical scattering-based measurements of different substances. In these experiments, changes in the concentration of a substance result in changes in scattering, and they are further seen in the optical signals. This theoretical background has been studied for noninvasive glucose monitoring.^{6,7} Increasing the glucose concentration decreases scattering and increases light penetration depth. In recent years, several optical methods, such as spatially resolved diffuse reflectance measurements and optical coherence tomography (OCT), have been used to study these changes in tissue-simulating phantoms and in tissues both *in vitro* and *in vivo*.⁸⁻¹¹ However, physiological glucose levels are in the range of 3 to 30 mM, which are far below the level of making the tissue transparent.

OCT is a high-resolution imaging technique based on an interferometer. After the invention of OCT in 1991,¹² it has been applied to several imaging applications.^{13,14} OCT is capable of detecting photons backscattered from different layers in the sample. Thus, changes in the scattering properties can be studied at different depths in the sample.

Address all correspondence to Matti Kinnunen, Optoelectronics and Measurement Techniques Laboratory, University of Oulu, Erkki Koiho-Kanttilan Katu, Oulu, Oulu FIN-90014 Finland; Tel: +358-8-553-7686; Fax: +358-8-553-2774; E-mail: matti.kinnunen@ee.oulu.fi

Investigation of the changes in a sample's scattering properties with OCT is based on analyzing the depth profile of an attenuating interference signal. Changing optical properties, i.e., in the case of adding glucose to the sample, induce changes in the slope value of a line fitted to the depth profile. The changes in the slope value can be thought to originate from changes in scattering in the following conditions: the scattering coefficient (μ_s) is much higher than the absorption coefficient (μ_a), and the slope-fitting regime is in the single-scattering part of the profile. Deeper in the sample, especially in a highly scattering medium, a more complicated model is preferred for extracting the value of μ_s .¹⁵

Optical scattering-based techniques, such as OCT, are based on the interaction of light with the object under study. The effect of glucose is measured through changes in the refractive index mismatch between scattering particles and the base medium, and hence in light scattering properties. Due to the indirect nature of the measurements, OCT is not specific for single glucose molecules, and hence all other effects that may change the scattering properties should be tightly controlled.¹⁶ It is easier to study the effects of different factors on the experiments in *in vitro* conditions. This is the reason for developing different tissue-simulating phantoms and complicated tissue models.¹⁷ Compared with *in vitro* experiments, *in vivo* measurements are confronted with different problems. These effects have been studied, e.g., by Larin et al.,¹⁶ and they include the effect of variation in the concentration of different tissue components, the physiological response of tissues, tissue heterogeneity, motion artifacts, and temperature.¹⁸ Recent progress in developing an OCT-based glucose sensor has been made in improving accuracy and in finding out other possible effects than glucose that would change the OCT signal's slope value.^{19–21} Quite recently, studies concerning possible enhancements of OCT to increase selectivity for single molecules have been published.²²

This work concentrates on the differences in the effect of glucose on the optical properties of different materials (Intralipid and skin). The differences between *in vitro* and *in vivo* experimental conditions are also considered.

2 Materials and Methods

2.1 Materials

Intralipid is an intravenous nutrient consisting of phospholipid micelles and water. The main components of Intralipid are purified soybean oil (100 g), purified lecithin (12 g), and glycerin (22.0 g). Phospholipid micelles generally have a spherical shape and their size varies between 25 and 675 nm. Their average size and standard deviation are 97 and 3 nm, respectively.²³ An Intralipid suspension is turbid and homogeneous, and it has largely been used as a phantom that mimicks the light-scattering properties of skin, although some of its optical properties (e.g., anisotropy and polarization) are quite different.^{24–26} The best correlation with human skin has been found with a 2% Intralipid concentration.²⁷ 2% Intralipid was used in the experiments. It was prepared by diluting 10% Intralipid (Fresenius Kabi AB, Uppsala, Sweden) with distilled water.

Fetuses 18.5 days old were taken out of a mouse uterus. Skin tissue samples were cut from their backs and put into a nutrient medium. The medium for skin culture consisted of

Dulbecco's Modified Eagle Medium (DMEM) solution (45 ml) (Gibco™, Invitrogen Ltd, Paisley, United Kingdom), fetal bovine serum (5 ml) (Gibco™), and penicillin streptomycin solution (0.5 ml) (Gibco™). The samples were placed in a plastic cuvette with a diameter of 34 mm (Greiner Bio-one Ltd, Stonehouse, United Kingdom) with a grid and a polycarbonate membrane filter (Whatman Maidstone, Kent, United Kingdom.) inside.²⁸

Mice C57BL were used in the *in vivo* studies. All the mice were males. The average weight of the animals was 20.6 g, with a standard deviation of 2 g. Altogether, ten experiments were conducted. Different concentrations of D(+)-glucose (C₆H₁₂O₆, M=198.17 g/mol, Merck, Eurolab) were used in all the experiments.

2.2 Optical Coherence Tomography Device

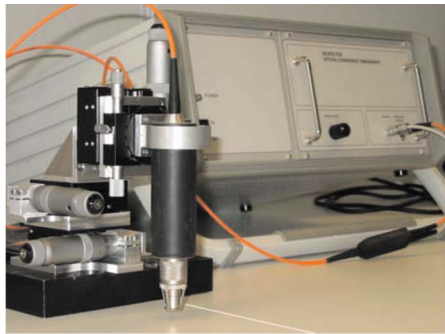
A commercial OCT system (manufactured by the Institute of Applied Physics, Nizhny Novgorod, Russia) was used in the studies. It uses a wavelength of 910 nm with resolutions of <10 μm for axial and lateral resolution in air. The spectrum width is 49 nm. The Doppler frequency of the OCT device is 1415 kHz. The OCT device was controlled with a PC via a USB channel. The signals were measured with an optical probe and saved on the computer. A scanner inside the optical probe scanned along the sample surface. The adjustable scanning range along the x and y axes was between 0 and 2.2 mm. The inner diameter of the optical fiber tip was 6 μm , the diameter of the cladding was $125 \pm 1 \mu\text{m}$, and the outside diameter was $245 \mu\text{m} \pm 5\%$. The size of the focus point was 8.4 μm when in the center area of the focal adjustment range of the probe, and with the magnification of the optics at 1.4. The numerical aperture of the optical fiber was in the range of 0.13 to 0.15. The lateral scanning range and the diameter of the probing beam increased proportionally to the magnification of the output lens.²⁹ The image acquisition speed of the OCT device was 1 image/s for an image size of 100×400 pixels (100 in the lateral and 400 in the depth direction). The setup used in the experiments is shown in Fig. 1.

2.3 Measurement Procedure and Signal Processing

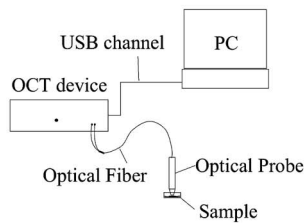
2.3.1 *In vitro*

The Intralipid samples were measured in a laboratory at normal room temperature. The samples were placed in a plastic cuvette with diameter of 34 mm (Greiner Bio-one). Glucose was added to the Intralipid samples in concentrations of 0, 27.78, 55.56, 166.67, and 277.78 mM (or 0, 500, 1000, 3000, and 5000 mg/dl, respectively). A wide range of concentrations was used because the effect of glucose on the optical properties of Intralipid is very weak. The 2% Intralipid samples with different amounts of glucose were measured with figure size of 200×500 pixels (1.100×1.931 mm). Each z -axial scan was averaged 20 times. Hence, the 1-D OCT signal profile contained 4000 scans. Each sample was measured five times, and the average and standard deviation were calculated with Microsoft® Excel 2002.

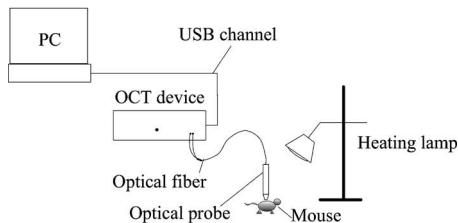
The *in vitro* studies with mouse skin samples were conducted in a warm room (+37°C). The samples were moved from the incubator to the warm room for the period of measurement. Glucose concentrations of 0 to 30 mM were used.



(a)



(b)



(c)

Fig. 1 Setup used in the experiments. (a) Image from the OCT device and probe, (b) schematic diagram of the setup used in the *in vitro* experiments, and (c) schematic diagram of the setup used in the *in vivo* experiments. (b) and (c) are from Refs. 28 and 30, respectively.

Some of the samples were measured after 24 h of culturing. The rest of the samples were cultured 4 days before the measurement. In this case, the culture medium was changed in the dishes after 2 days. Glucose was added to the dish with a pipette, and the waiting period before the next measurement varied from 30 min to 1 h in different sample series. In this set of measurements, the size of the OCT imaging was 100×400 pixels (0.66×1.545 mm). The z -axial scans were averaged ten times, and thus the averaged depth profile contained 1000 scans. Each sample was measured ten times and the average values and the standard deviations were calculated with Microsoft® Excel 2002.²⁸

2.3.2 *In vivo*

The *in vivo* measurements were taken in a laboratory. The mice were fasted for more than 6 h before the measurements were taken. Ratanest was used to anesthetize the mice in the beginning. Ratanest consists of Hypnorm (fentanyl citrate 0.315 mg/ml and fluanisone 10 mg/ml, VetaPharma Limited, Leeds, United Kingdom) and Dormicum (midazolam 5 mg/ml, Roche Oy, Espoo, Finland). Both were diluted with

water at a ratio of 1:1, and then mixed with each other. This has been found to be an appropriate anesthetic agent for anesthetizing mice. Hair was removed from the beneath the OCT probe. To prevent cooling of the animals, the mice were placed on a table, under a warm lamp, during the measurements. After measuring the zero level reference value, a glucose solution with a concentration of 555.56 mM (equals 10 g/dl) was injected into the mice (i.p.). The glucose was injected according to the weight of the animals (1 ml/100 g).

The time for baseline registering of the OCT slope value varied from 15 to 40 min at the beginning. The zero-minute blood glucose value was measured before the glucose was injected (i.p.) into the abdominal cavity at zero minutes. The OCT signals were registered about 2 h after the glucose injection. The reference values were measured at 0, 15, 30, 60, 90, and 120 min from the beginning of the injection. The blood glucose values were measured with an Ascensia Elite™ XL blood glucose meter. Each control measurement required 2 μ l of blood, which was taken from the feet of the mice.

The OCT images were registered continuously during the experiment. An image [size 300×400 pixels (1.126×1.288 mm), 300 in the lateral and 400 in the depth direction] was saved on the computer every 30 s. The depth scans were averaged seven times. The images were processed afterward using a Matlab application. Signal processing contained the following steps: averaging of 300 separate scans, fitting the slope to an appropriate depth, extracting the slope values of the fitted lines, and finally, averaging five slope values.

3 Results and Discussion

The three samples used in the studies, Intralipid, skin tissue samples, and mice *in vivo*, have different optical properties and physical structures. Figures 2(a) and 2(b) show a typical OCT image and a 1-D depth profile from Intralipid, respectively. Figures 2(c) and 2(d) show a typical OCT image and a 1-D depth profile from the skin tissue sample, respectively. Figures 2(e) and 2(f) show a typical OCT image and a 1-D depth profile from the mouse skin *in vivo*. Physical depths were calculated by dividing the optical depth values with the average refractive index of the sample. A refractive index value of 1.34 was used for 2% Intralipid in Figs. 2(a) and 2(b), a refractive index value of 1.4 was used for the skin tissue sample in Figs. 2(c) and 2(d), and for mouse skin in Figs. 2(e) and 2(f).^{22,23}

Figures 2(a) and 2(b) show that Intralipid is quite a homogeneous and turbid material, whereas the refractive index distribution has more variation in the studied tissue samples [Figs. 2(c) and 2(d)]. The *in vivo* results show the highest backscattering intensity when measured with OCT, but also rapid attenuation as a function of depth. The peaks at the beginning of the images (left side) result from reflection from the sample's surface.

Different concentrations of glucose were added to the samples to study possible differences in matching of the refractive indices in different samples, and hence changes in the optical scattering properties. Figure 3 shows focused views of the fitted lines on the OCT signal depth profiles in different samples with two different glucose concentrations. Physical depths were calculated by dividing the optical depth values with the average refractive index of the sample. A refractive

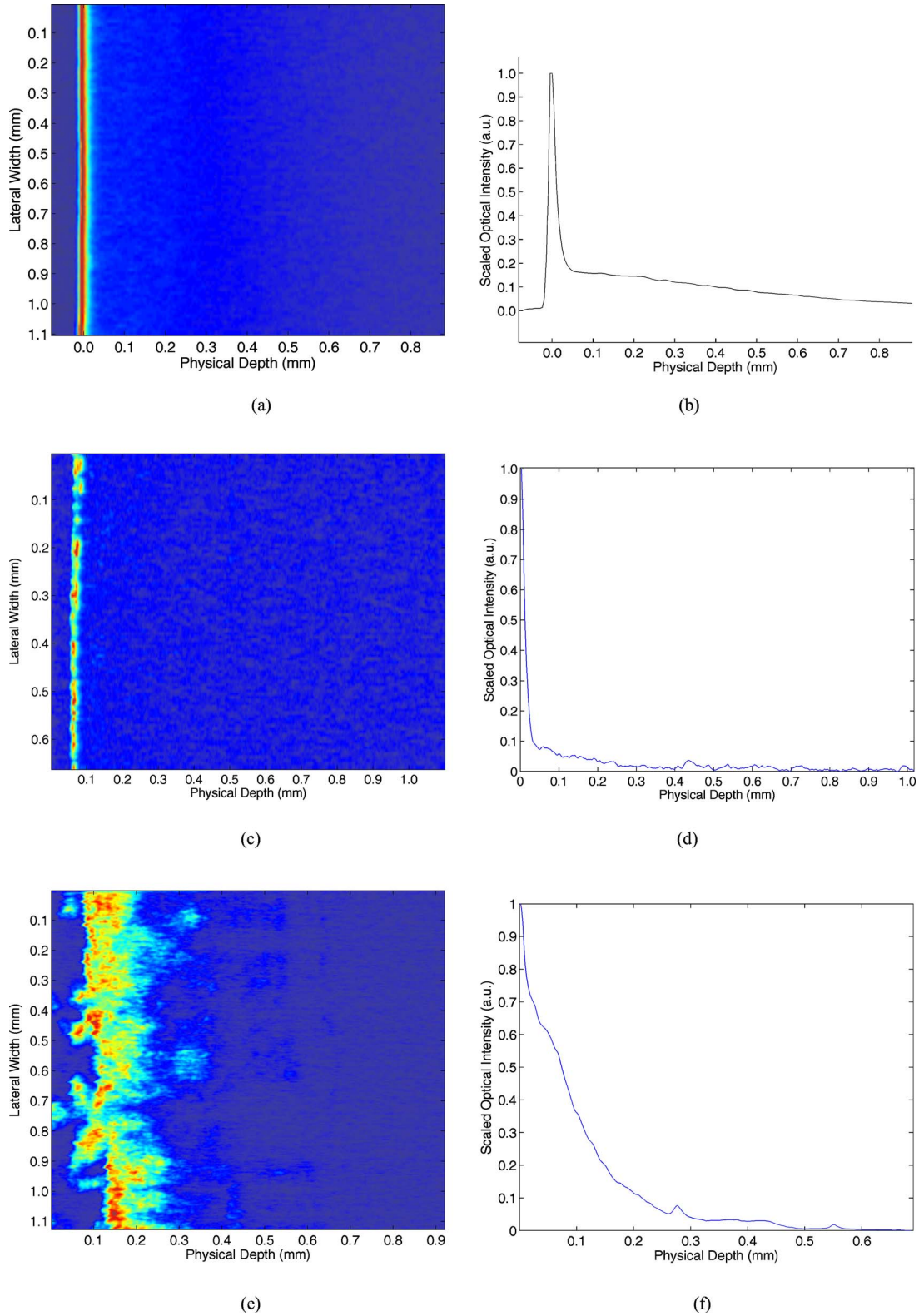


Fig. 2 (a) OCT image and (b) averaged depth profile from 2% Intralipid. (c) OCT image and (d) averaged depth profile from the skin tissue sample: and (e) OCT image and (f) averaged depth profile from mouse skin tissue *in vivo*.

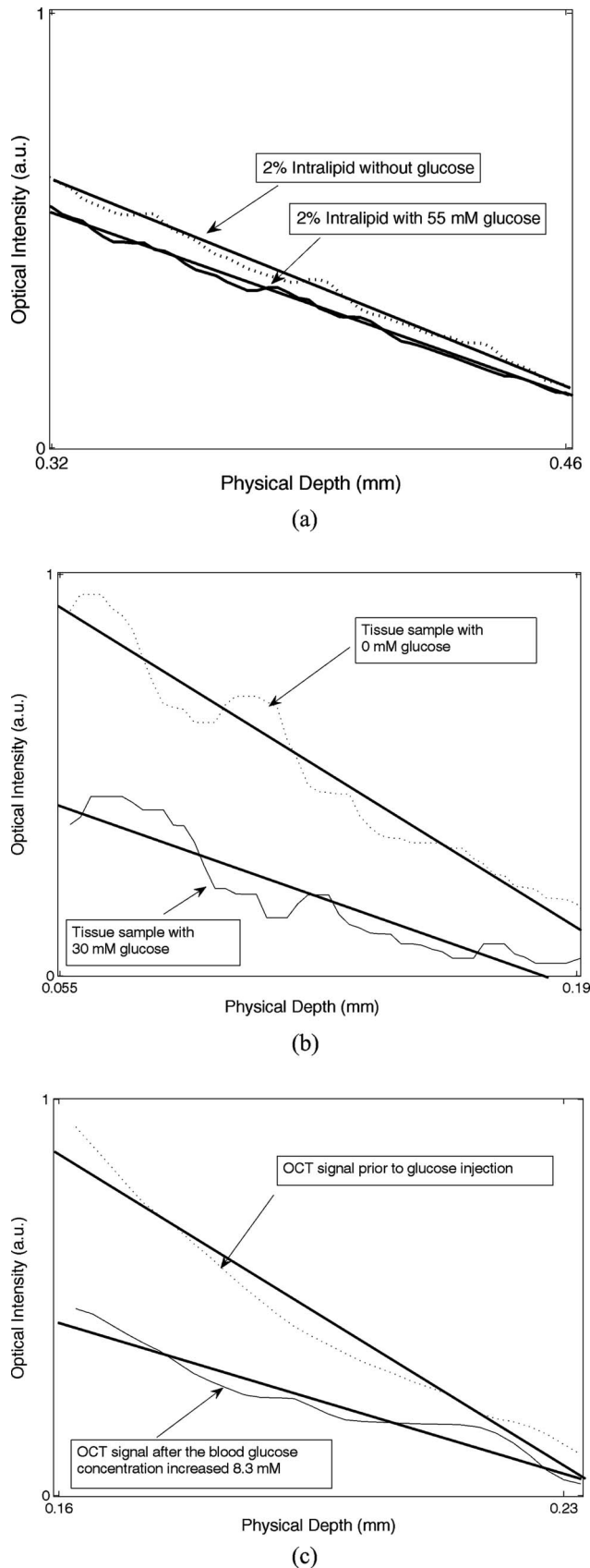


Fig. 3 Fitting of a straight line on the OCT signal profiles at two different glucose concentrations from (a) 2% Intralipid, (b) a skin tissue sample, and (c) mouse skin *in vivo*.

index value of 1.34 was used for 2% Intralipid in Fig. 3(a), and a refractive index value of 1.4 was used for the mouse skin tissue sample in Fig. 3(b) and for mouse skin in Fig. 3(c).^{2,23}

In the Intralipid samples, the slope values were determined by fitting the slope on the most linear part of the attenuation curve after the sample surface [Fig. 3(a)]. This was also true for the skin tissue samples *in vitro* [Fig. 3(b)].²⁸ The effect was smallest in the Intralipid samples, whereas the matching effect was larger in the real tissue. This indicates that optical clearing with glucose would also be more obvious *in vivo*. In the *in vivo* measurements, the slope values were determined at the place where the glucose-induced change in the slope value was at a maximum [Fig. 3(c)]. This was found to be in the dermis part of the skin, where the network of small capillaries is located. The value of 2.7 %/mM is an average of four measurements: 1.6, 1.077, 3.36, and 4.85%, which were recently published in Ref. 30. The correlation coefficients of those measurements were 0.24, 0.75, 0.86, and 0.60, respectively. The very pure value of 0.24 was due to some unexpected changes in the slope values at the end of the experiment.

Table 1 shows the average glucose-induced changes in the OCT signal slope value obtained from the different samples. The *in vitro* tissue experiments consisted of measurements of five different samples. Possible reasons for the different effect of glucose could be the different refractive indices of the scattering centers in Intralipid and in skin tissue. The refractive index of soybean particles is ≈ 1.463 , and of water ≈ 1.33 . In tissue samples, $n \approx 1.40$ for mitochondria, 1.46 for collagen fibers, and ≈ 1.362 for extracellular fluid. Assuming seventy percent of the dry weight of skin consists of collagen fibers and approximating the rest to be formed by other components with $n=1.40$, it is possible to get the value of $n=0.7 \times 1.46 + 0.3 \times 1.4 = 1.442$ for skin tissue. For the nutrition medium, n was supposed to be the same as for water.^{2,23,31,32} This gives the refractive index difference between the bulk medium and scattering particles of $\Delta n \approx 1.442 - 1.362 = 0.08$ for skin tissue *in vivo*, $\Delta n \approx 1.442 - 1.33 = 0.112$ for skin samples *in vitro*, and $\Delta n \approx 1.463 - 1.33 = 0.133$ for 2% Intralipid. Possible errors may be induced into the calculations when assuming the refractive index of the nutrition medium to be 1.33 instead of a combination of the refractive indices of the nutrition medium and intracellular fluid. Moreover, alteration of the sizes of the scattering centers and cells by contracting or swelling has to be taken into account in the skin experiments.⁴

The skin samples and the skin *in vivo* have a layered structure. The main layers in the mouse skin are the epidermis and dermis, with thicknesses of a few dozen micrometers and between 170 to 500 μm , respectively,^{33,34} *in vivo*. They differ largely from the Intralipid suspensions. Although Intralipid quite closely imitates the properties of skin in transmittance and reflectance measurements,²⁶ there are no different layers observed in the measured OCT images. In Intralipid, the scattering particles have an almost spherical shape, whereas there are many kinds of components with varying shapes in skin (e.g., collagen fibers, cell nucleus, mitochondria, etc.). The results also show that backscattering of photons is much stronger in real tissue *in vivo* than *in vitro*. One explanation is

Table 1 Average glucose-induced changes in the OCT signal slope value in Intralipid and skin samples *in vitro*, and mouse skin *in vivo*.

	Average change in slope / mM	Standard deviation	Number of measurements/samples	Reference
Intralipid				
2 % IL	0.07 % / mM	0.004	5	28
5 % IL	0.3 % / mM	0.011	5	28
Fetal skin, <i>in vitro</i>	1.37 % / mM	0.46	5	28
Mouse, <i>in vivo</i>	2.7 % / mM	1.7	4	30

the lack of blood in the tissue samples, but in the *in vivo* experiments, blood is present.

The basic setup for glucose injection is different in the *in vitro* and *in vivo* experiments. In the *in vitro* case, glucose was added to the dish and the solution was mixed a little. In these experiments, the glucose was thought to be distributed smoothly in the sample after a time period of 15 to 30 min after glucose addition. On the contrary, in the *in vivo* experiments, the glucose was diffused into the tissue from blood. Thus, the original place where the glucose load penetrated the sample was different. Both methods were different from those used in the experiments conducted by Wang and Tuchin,³ where intradermal injection was used. Intradermal injection was used because the epidermis has very slow permeability to glucose.³

The place of measurement has more effect on the measurements in the skin than in the Intralipid. This is due to the inhomogeneous structure of the skin sample surface. Measurement at different places on the rough sample surface leads to a large standard deviation in the measurements. However, the skin tissue samples stayed still during the measurements. The situation is different in the experiments *in vivo*, where the motion of the mice caused distortions during the 2-h measurement period. The movements took place especially in the cases where blood samples were taken from the feet of the mice to measure blood glucose control values, and when the effect of the anesthetic drug weakened and more of the drug was injected. The motion artifacts were corrected afterward.

The measurement conditions, such as temperature, humidity, and CO₂ content, also affect the results. The mouse skin samples were measured in a warm room (+37°C). This diminished the effect of changing temperature during the experiments. The measurement time in the *in vitro* measurements was minimized to only about ten seconds for one image to diminish the effect of decreasing CO₂ content while the samples were outside the incubator. Because the optical system of the measurement probe has a curved focus plane, the width of the scanned image was decreased from the maximum to avoid harmful effects on the OCT signal depth profile and to increase the accuracy of the experiments.

A comparison of the glucose-induced changes in the Intralipid and other *in vitro* measurements (wavelength is 1310 nm) shows quite good comparability. The glucose-induced changes vary in the range of 0.023%/mM for poly-

styrene microspheres *in vitro*⁹ to 2.5 %/mM in Yucatan Micropigs,³⁵ 3.3 %/mM for rabbit ear,¹⁶ and 3.42%/mM for human skin¹¹ *in vivo*. The *in vivo* results from mice are in the same range as the other *in vivo* experiments. The glucose values *in vitro* from the skin tissue samples are in the middle of these two categories.

4 Conclusions

The structures of the studied samples, Intralipid, fetal skin tissue samples, and mouse skin tissue *in vivo*, differ from each other because Intralipid has spherical scattering particles with varying size and homogeneous particle distribution, while skin tissue consists of several components with different diameters and shapes and a layered structure. OCT signals from the studied samples show that scattering in the backward direction is stronger from skin tissue *in vivo* than from skin samples *in vitro*. Glucose is found to have the most pronounced effect in *in vivo* conditions, and the smallest effect in 2% Intralipid. This can partly be explained by the refractive index differences between the bulk medium and scattering particles ($\Delta n \approx 0.08$ for skin tissue *in vivo*, $\Delta n \approx 0.112$ for skin samples *in vitro*, and $\Delta n \approx 0.133$ for Intralipid).

These results confirm that a commercial OCT device, designed for imaging purposes, is capable of detecting glucose-induced changes in scattering in different types of samples in very well-controlled conditions. Moreover, cell cultured tissue samples seem to be a viable, although not most stable, option when developing optical sensing techniques from a phantom base toward *in vivo* conditions. However, if more parameters change simultaneously, this analysis method is not accurate enough. In that case, quantification of the glucose concentration cannot be made from one measurement. Thus, simultaneous measurements with different techniques or improved glucose selectivity with OCT are needed.

Acknowledgments

The authors would like to thank Tiina Jokela, Sirpa Tausta, Annakaisa Herrala, and Erkki Alarousu as well as the personnel of the Laboratory Animal Centre and the Department of Medical Biochemistry and Molecular Biology of the University of Oulu for help and discussions during the experiments. In addition, Infotech Oulu is acknowledged for giving financial support during the experiments.

References

1. V. V. Tuchin, I. L. Maksimova, D. A. Zimnyakov, I. L. Kon, A. H. Mavlutov, and A. A. Mishin, "Light propagation in tissues with controlled optical properties," *J. Biomed. Opt.* **2**(4), 401–417 (1997).
2. V. V. Tuchin, *Tissue Optics, Light Scattering Methods and Instruments for Medical Diagnosis*, Tutorial Texts in Optical Engineering TT38, SPIE Press, Bellingham, WA 2000.
3. R. K. Wang, and V. V. Tuchin, "Enhance light penetration in tissue for high resolution optical imaging techniques by the use of biocompatible chemical agents," *Proc. SPIE* **4956**, 314–319 (2003).
4. F. Zhou and R. K. Wang, "Theoretical model on optical clearing of biological tissue with semipermeable chemical agents," *Proc. SPIE* **5530**, 215–221 (2004).
5. V. V. Tuchin, "Optical clearing of tissues and blood using the immersion method," *J. Phys. D* **38**, 2497–2518 (2005).
6. M. Kohl, M. Cope, M. Essenpreis, and D. Böcker, "Influence of glucose concentration on light scattering in tissue-simulating phantoms," *Opt. Lett.* **19**, 2170–2172 (1994).
7. M. Kohl, M. Essenpreis, and M. Cope, "The influence of glucose concentration upon the transport of light in tissue-simulating phantoms," *Phys. Med. Biol.* **40**, 1267–1287 (1995).
8. J. T. Bruulsema, J. E. Hayward, T. J. Farrell, M. S. Patterson, L. Heinemann, M. Berger, T. Koschinsky, J. Sandahl-Christiansen, H. Orskov, M. Essenpreis, G. Schmelzeisen-Redeker, and D. Böcker, "Correlation between blood glucose concentration in diabetics and noninvasively measured tissue optical scattering coefficient," *Opt. Lett.* **22**, 190–192 (1997).
9. K. V. Larin, T. V. Ashitkov, I. Larina, I. Petrova, M. Eledrisi, M. Motamedi, and R. O. Esenaliev, "Optical coherence tomography and noninvasive blood glucose monitoring: a review," *Proc. SPIE* **5474**, 285–290 (2004).
10. R. O. Esenaliev, K. V. Larin, I. V. Larina, and M. Motamedi, "Non-invasive monitoring of glucose concentration with optical coherence tomography," *Opt. Lett.* **26**, 992–994 (2001).
11. K. V. Larin, M. Motamedi, M. S. Eledrisi, and R. O. Esenaliev, "Non-invasive blood glucose monitoring with optical coherence tomography. a pilot study in human subjects," *Diabetes Care* **25**, 2263–2267 (2002).
12. D. Huang, E. A. Swanson, C. P. Lin, J. S. Schuman, W. G. Stinson, W. Chang, M. R. Hee, T. Flotte, K. Gregory, C. A. Puliafito, and J. G. Fujimoto, "Optical coherence tomography," *Science* **254**, 1178–1181 (1991).
13. J. M. Schmitt, "Optical coherence tomography (OCT): a review," *IEEE J. Sel. Top. Quantum Electron.* **5**, 1205–1215 (1999).
14. M. Kinnunen, Z. Zhao, and R. Myllylä, "Comparison of the pulsed photoacoustic technique and the optical coherence tomography from the viewpoint of biomedical sensing," *Proc. SPIE* **5946**, 468–480 (2005).
15. M. Kinnunen and R. Myllylä, "Measuring changes in the scattering properties of Intralipid at different depths with optical coherence tomography," *Proc. SPIE* **6536**, 65360N (2007).
16. K. V. Larin, M. Motamedi, T. V. Ashitkov, and R. O. Esenaliev, "Specificity of noninvasive blood glucose sensing using optical coherence tomography technique: a pilot study," *Phys. Med. Biol.* **48**, 1371–1390 (2003).
17. B. W. Pogue and M. S. Patterson, "Review of tissue simulating phantoms for optical spectroscopy, imaging, and dosimetry," *J. Biomed. Opt.* **11**, 041102 (2006).
18. O. S. Khalil, "Non-invasive glucose measurement technologies: an update from 1999 to the dawn of the new millennium," *Diabetes Technol. Therapeut.* **6**, 660–697 (2004).
19. R. V. Kuranov, V. V. Sapozhnikova, D. S. Prough, I. Cicenaite, T. Wegeng, and R. O. Esenaliev, "Influence of external factors on blood glucose sensing with optical coherence tomography," presented at *Optical Diagnostics and Sensing VII, Proc. SPIE* **6445**, 644523 (2007).
20. R. V. Kuranov, V. V. Sapozhnikova, D. S. Prough, I. Cicenaite, and R. O. Esenaliev, "In vivo study of glucose-induced changes in skin properties assessed with optical coherence tomography," *Phys. Med. Biol.* **51**, 3885–3900 (2006).
21. V. V. Sapozhnikova, D. Prough, R. V. Kuranov, I. Cicenaite, and R. O. Esenaliev, "Influence of osmolytes on *in vivo* glucose monitoring using optical coherence tomography," *Exp. Biol. Med.* **231**, 1323–1332 (2006).
22. C. Yang, M. A. Choma, L. E. Lamb, J. D. Simon, and J. A. Izatt, "Protein-based molecular contrast optical coherence tomography with phytochrome as the contrast agent," *Opt. Lett.* **29**, 1396–1398 (2004).
23. H. J. van Staveren, C. J. M. Moes, J. van Marle, S. A. Prahl, and M. J. C. van Gemert, "Light scattering in Intralipid-10% in the wavelength range of 400–1100 nm," *Appl. Opt.* **30**, 4507–4514 (1991).
24. S. T. Flock, S. L. Jacques, B. C. Wilson, W. M. Star, and M. J. C. van Gemert, "Optical properties of Intralipid: a phantom medium for light propagation studies," *Lasers Surg. Med.* **12**, 510–519 (1992).
25. V. Sankaran, K. Schönenberger, J. T. Walsh Jr, and D. J. Maitland, "Polarization discrimination of coherently propagating light in turbid media," *Appl. Opt.* **38**, 4252–4261 (1999).
26. K. J. Jeon, I. D. Hwang, S. Hahn, and G. Yoon, "Comparison between transmittance and reflectance measurements in glucose determination using near infrared spectroscopy," *J. Biomed. Opt.* **11**, 014022 (2006).
27. T. L. Troy and S. N. Thennadil, "Optical properties of human skin in the near infrared wavelength range of 1000 to 2200 nm," *J. Biomed. Opt.* **6**(2), 167–176 (2001).
28. M. Kinnunen, R. Myllylä, T. Jokela, and S. Vainio, "In vitro studies toward noninvasive glucose monitoring with optical coherence tomography," *Appl. Opt.* **45**, 2251–2260 (2006).
29. N. Ayari, A. Popov, M. Kinnunen, R. Myllylä, and F. Zhang, "Sensing an aqueous Intralipid suspension with optical coherence tomography: reconstruction of scattering coefficients," *Proc. SPIE* **6536**, 65360M (2007).
30. M. Kinnunen, S. Tausta, R. Myllylä, and S. Vainio, "Monitoring changes in the scattering properties of mouse skin with optical coherence tomography during an *in vivo* glucose tolerance test," *Proc. SPIE* **6535**, 65350B (2007).
31. J. Beuthan, O. Minet, J. Helfmann, M. Herrig, and G. Müller, "The spatial variation of the refractive index in biological cells," *Phys. Med. Biol.* **41**, 369–382 (1996).
32. R. Drezek, A. Dunn, and R. Richards-Kortum, "Light scattering from cells: finite-difference time-domain simulations and goniometric measurements," *Appl. Opt.* **38**, 3651–3661 (1999).
33. L. J. Bussau, L. T. Vo, P. M. Delaney, G. D. Papworth, D. H. Barkla, and R. G. King, "Fibre optic confocal imaging (FOCI) of keratinocytes, blood vessels and nerves in hairless mouse skin *in vivo*," *J. Anat.* **192**, 187–194 (1998).
34. L. Azzi, M. El-Alfy, C. Martel, and F. Labrie, "Gender differences in mouse skin morphology and specific effects of sex steroids and dehydroepiandrosterone," *J. Invest. Dermatol.* **124**, 22–27 (2005).
35. K. V. Larin, T. V. Ashitkov, I. V. Larina, I. Y. Petrova, M. Eledrisi, M. Motamedi, and R. O. Esenaliev, "Optical coherence tomography technique for non-invasive blood glucose monitoring: phantom, animal, and human studies," *Proc. SPIE* **4619**, 157–164 (2002).